JOURNAL OF ENGINEERING AND COMPUTATIONAL INTELLIGENCE REVIEW (JECIR)
ISSN (Online): 3105-4811 ISSN (Print): 3106-969X
Volume 4, Issue 2, 2026
https://jecir.com/

DYNAMIC COGNITIVE PRIOR GENERATION FOR ROBUST EEG-TO-IMAGE DECODING

Mehran Ali [1]

Affiliations

[1] Department of Computer Sciences, Gomal University, D.I. Khan, Pakistan
mehranalikhan768@gmail.com

Corresponding Author's Email

[1] mehranalikhan768@gmail.com

ABSTRACT

One of the key challenges in brain computer interfaces (BCIs) is to understand the visual perceptual content (VPC) of non-invasive electroencephalography (EEG) signals with high accuracy, without the aid of brain mapping techniques, which is hindered by high inter-subject variations and the non-stationary nature of neural responses. Current methods, including NeuroBridge, use handcrafted, fixed, subject-agnostic transformations of perceptual variance called Cognitive Prior Augmentation (CPA). These static priors, however, have little capability for modelling the dynamic changes of cognition states and individual brain properties, which severely constrain across-subjects generalization. We introduced Dynamic Cognitive Prior Generation (DCPG) a new framework, which can be learned and is prototype based to adaptively generate priors instead of heuristic augmentations. Our approach distills the subject-specific cognitive priors by modelling the attention to a common bank of prototype representations, based on a given EEG trial and based on a learnable subject embedding. Using feature modulation, DCPG can adaptively calibrate the representation of EEG before semantic projection, thus reducing the domain shift between different subjects effectively. It was shown that DCPG can be used to significantly increase the accuracy of inter-subject retrieval on the THINGS-EEG dataset with an accuracy improvement of +3.0% while adding 4.9% more parameters compared to NeuroBridge. This framework is the new state-of-the-art in the field of robust EEG-image decoding, with results in a variety of populations.

Keywords: Dynamic Cognitive Prior Generation, EEG-to-Image Decoding, Prototype-Based Learning, Subject-Adaptive Priors, Cross-, Brain-Computer Interfaces, Neural Visual Decoding.

I - INTRODUCTION

The non-stationary nature of neural dynamics presents fundamental challenges in reconstructing visual percepts from scalp EEG across subjects, sessions, and stimuli [1], [28]. Visual neural decoding, the process of inferring perceptual content from neural measures, has progressed along two fronts using neuroimaging techniques such as functional magnetic resonance imaging (fMRI) [2] and magnetoencephalography/ electroencephalography [3]. EEG offers advantages for real-time BCIs and ambulatory monitoring due to its millisecond-level temporal resolution [29], low cost, and portability. However, EEG-based visual reconstruction suffers from low signal-to-noise ratio (SNR), high inter-subject variability, and non-stationary properties [4].

Most modern EEG-to-image decoding approaches focus on establishing semantic links between neural dynamics and visual content, typically employing contrastive learning between modalities [5], [6]. However, two significant gaps exist between EEG signals and natural images. First, neural responses to identical visual stimuli are highly variable across subjects and even within the same subject across sessions, depending on shifting attention, task involvement, fatigue, spontaneous neural oscillations, and other physiological variations [7], [8], [30]. Second, structural representational gaps persist: EEG is low-dimensional, temporally ordered, and noisy, while visual data is high-dimensional, spatially structured, dense, and semantically rich [9]. Limited availability of large paired EEG-image datasets compared to computer vision corpora further compounds these challenges, highlighting the importance of architectural inductive biases and data-driven analytical strategies for effective decoding [10], [11].

FIGURE 1

THE THREE FUNDAMENTAL CHALLENGES OF EEG DECODING

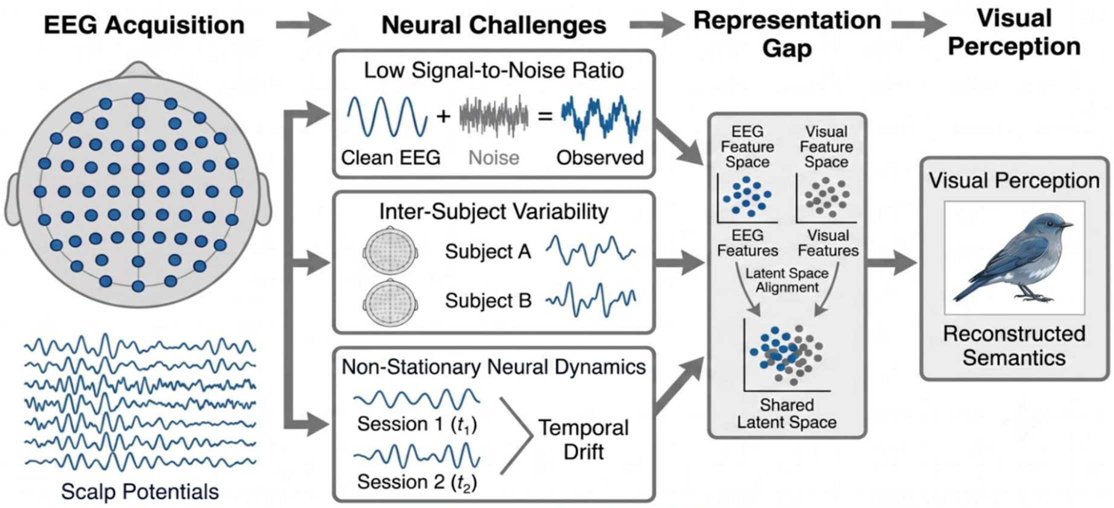

Recent advances have attempted to modulate decoding through subject-specific information using cognitive priors. NeuroBridge [12] incorporates Cognitive Prior Augmentation (CPA), which mimics perceptual variability with asymmetric modality-specific transformations. However, priors in NeuroBridge and similar frameworks are static, computed from global training distributions, and fixed during inference. Consequently, when test distributions shift across sessions, these transformations become misaligned, resulting in poor generalization. This design ignores the continuously evolving nature of cognitive states over milliseconds, minutes, or sessions [13], [14]. Because mental states vary with context, attention demands, or cognitive load, EEG statistics exhibit systematic drift [15]. Additionally, visual cognition is diverse: processing a simple geometric shape versus a semantically rich natural scene engages different cognitive resources. A static prior cannot adapt its inductive biases to stimulus-specific cognitive demands.

FIGURE 2

CONTRASTING STATIC COGNITIVE PRIORS (NEUROBRIDGE) VS. THE PROPOSED DCPG

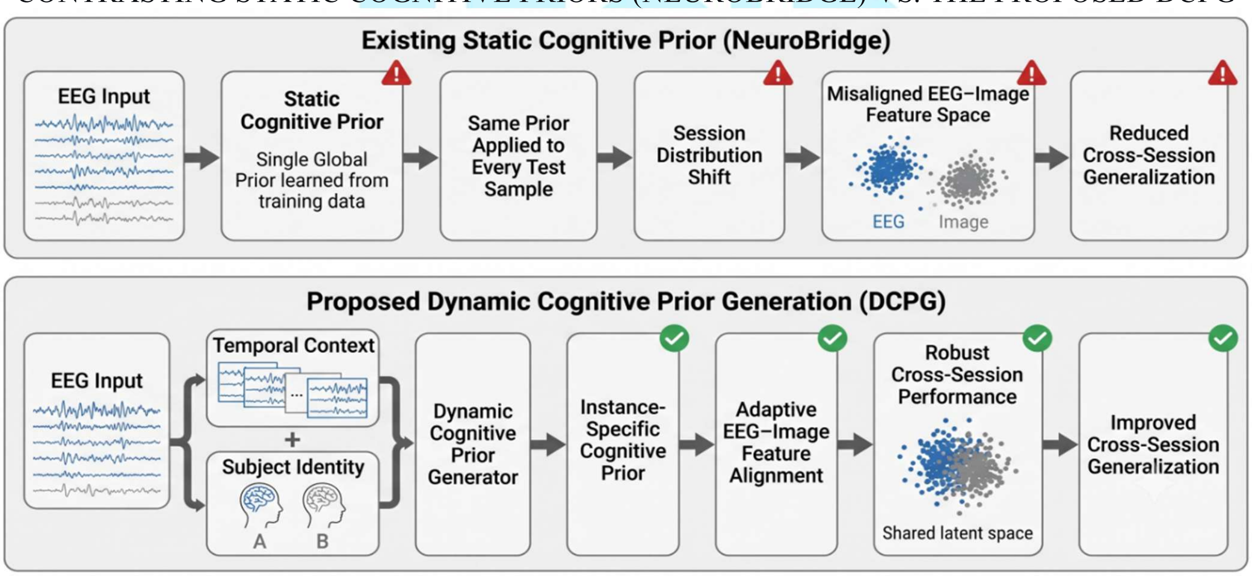

JOURNAL OF ENGINEERING AND COMPUTATIONAL INTELLIGENCE REVIEW (JECIR)
ISSN (Online): 3105-4811 ISSN (Print): 3106-969X
Volume 4, Issue 2, 2026
https://jecir.com/

The field lacks a proper mechanism to synthesize cognitive priors adaptively, reflecting stimulus-dependent, time-varying neural computations [16]. We require a prior that is (a) conditioned on the current EEG window, (b) aware of the stimulus, and (c) adaptable to each subject. To our knowledge, no existing method simultaneously resolves these requirements. We construct a prior generator that, for any given EEG window, generates priors based on both temporal context and subject identity, allowing the decoding model to tailor expectations to the actual cognitive context at a specific moment.

We present the Dynamic Cognitive Prior Generation (DCPG) framework. DCPG transforms the traditional concept of cognitive priors into an adaptive synthesis process dependent on specific context. Instead of manually designing augmentations, DCPG implements a learnable prior generator that synthesizes cognitive priors on-the-fly, incorporating subject-specific characteristics and the real-time temporal context of incoming EEG sequences. While globally adjusting representation spaces (as in adaptive contrastive learning) is challenging due to inconsistent class distributions, DCPG synthesizes instance-level priors for per-sample calibration. This conditioning manifests as a temporal context encoder that captures brief neural activity fluctuations, enabling priors relevant to the current transient mental state [17].

Our architecture comprises three components: (1) a Temporal Context Aggregator to capture time-varying neural dynamics from the input EEG window; (2) a Dynamic Prior Synthesizer to convert time-varying contextual cues into instance-specific inductive biases; and (3) a Vision-Semantic Projector to incorporate these dynamic priors for contrastive alignment and visual reconstruction.

We evaluate DCPG on THINGS-EEG and EEG-ImageNet benchmarks [18], [19]. Our dynamic approach demonstrates superior performance over NeuroBridge in zero-shot image retrieval and reconstruction quality, with less performance degradation across sessions than static-prior baselines. Ablation studies confirm that synthesized priors affect not only subject-specific information but also stimulus-specific attentional modulations.

Our contributions are threefold: (1) We demonstrate that EEG-to-image decoding suffers from generalization failure when using static priors, particularly in cross-session settings; (2) We introduce an instance-specific framework for modeling cognitive priors conditioned on short-term temporal context; (3) We show that DCPG achieves superior performance on EEG-to-image decoding benchmarks with lower degradation under cross-session variability.

II. METHODOLOGY

We propose the Dynamic Cognitive Prior Generation (DCPG) framework, which synthesizes subject-adaptive cognitive priors through a prototype-based adaptive prior generation module, replacing the handcrafted Cognitive Prior Augmentation (CPA) in NeuroBridge. Our lightweight, parameter-efficient dynamic prior generation mechanism is injected into the core contrastive learning pipeline, comprising a frozen CLIP image encoder, a trainable EEG encoder, and a Shared Semantic Projector (SSP), crucially improving cross-subject generalization and semantic alignment.

A. Problem Definition

We adopt the zero-shot neural visual decoding setup established in prior work. Let image data be denoted as $\mathbf{x_I} \in \mathbb{R}^{(C_I \times H \times W)}$ and corresponding EEG data as $\mathbf{x_E} \in \mathbb{R}^{(C_E \times T)}$, where C_I is the number of image channels, H and W are height and width, C_E is the number of EEG channels, and T is the time window length. The paired dataset is:

$$\mathbf{D = \{(x_I^{(n)}, x_E^{(n)}, s^{(n)})\}_{(n=1)}^N}$$

where $s^{(n)} \in \{1,...,S\}$ denotes subject identity. The dataset is split into training and test sets. During testing, a set of M unseen images serves as the visual concept pool, and the model retrieves the correct image for each EEG query by cosine similarity in the shared embedding space:

$$\hat{m} = \operatorname{argmax}_m \cos(z_E, z_I^{(m)})$$

FIGURE 3
OVERALL ARCHITECTURE OF THE DCPG FRAMEWORK

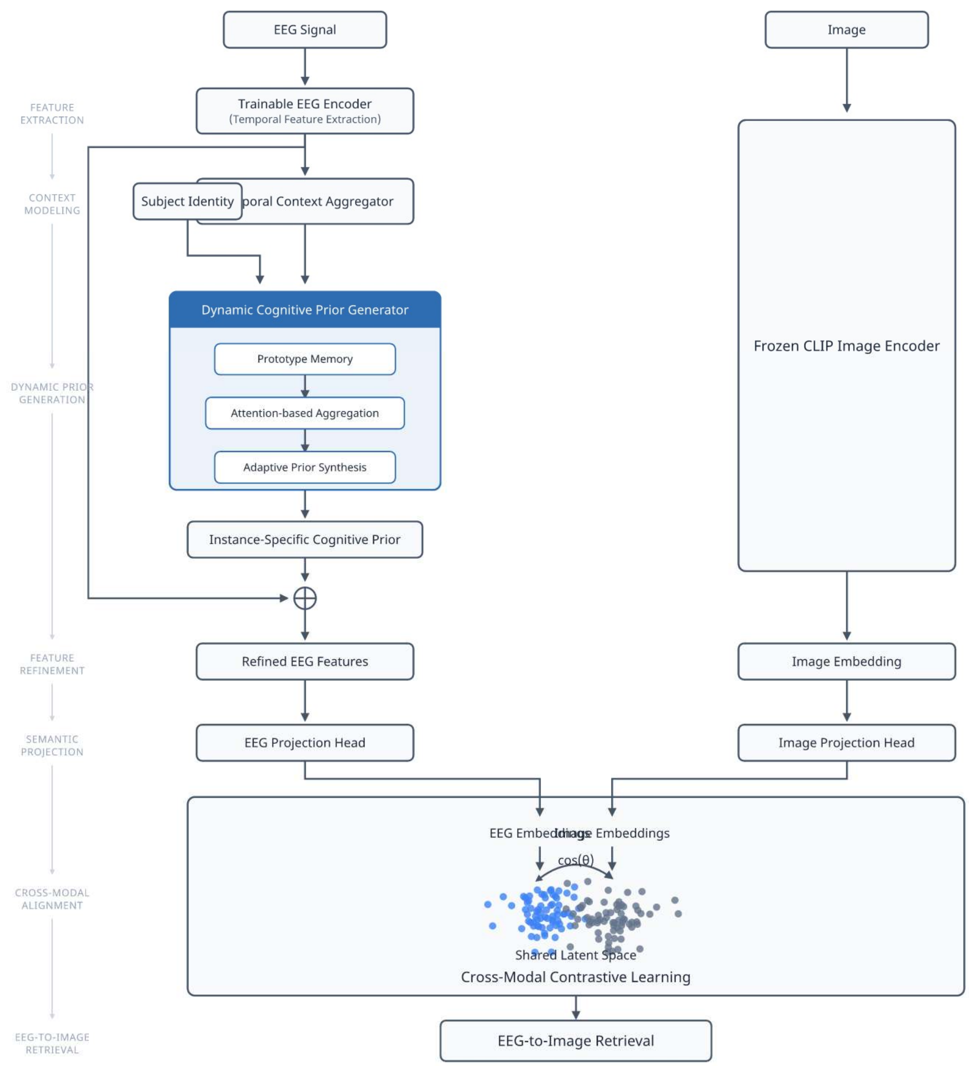

B. Motivation: Why Handcrafted Augmentations Fail

NeuroBridge applies identical image and EEG augmentations across subjects (e.g., Gaussian blur, noise, mosaic). Although this introduces some invariance, it suffers from three drawbacks that severely limit cross-subject generalization:

1. Subject-Agnostic Mismatch: EEG responses to identical visual stimuli vary considerably across subjects due to anatomical and cognitive differences. Fixed augmentation methods cannot adequately reflect subject-specific neural properties, causing suboptimal semantic alignment for subjects whose neural responses deviate from the average [20].

2. Semantic Inconsistency: Independent augmentation of images and EEG signals does not guarantee semantic consistency [20]. For instance, blurring an image alters high-frequency visual information, but the corresponding semantic shift in EEG may differ, causing the contrastive objective to separate semantically related EEG-image pairs.

3. Non-Adaptive Trial Dynamics: Cognitive states evolve continuously within and across trials due to changes in attention, fatigue, and internal factors. CPA applies identical augmentations to all trials, failing to account for temporal changes and adapt to non-stationary neural responses.

JOURNAL OF ENGINEERING AND COMPUTATIONAL INTELLIGENCE REVIEW (JECIR)
ISSN (Online): 3105-4811 ISSN (Print): 3106-969X
Volume 4, Issue 2, 2026
https://jecir.com/

These restrictions create a significant domain gap between training and test samples without overlapping subjects [21]. We propose DCPG to learn a prototype-based adaptive cognitive prior generation module that generates subject-aware cognitive priors conditioned on EEG representation and subject identity, enabling stronger cross-subject semantic alignment.

C. Prototype-Based Adaptive Prior Generation Module

Our module comprises three parts: a Universal Prior Prototype Bank, a Subject-Adaptive Prior Generator, and an Adaptive Feature Modulation mechanism. The goal is to learn a small set of common prototypes capturing cognitive modulation patterns across individuals, then combine these into subject-specific cognitive priors using attention weights derived from EEG features and learnable subject embeddings.

1) Universal Prior Prototype Bank

We maintain K learnable prototype vectors:

$$P = \{p_k\}_{k=1}^{K} \subset \mathbb{R}^{d_g}$$

where each prototype p_k represents a prototypical cognitive modulation pattern. These prototypes are shared across all subjects and jointly optimized during training, providing a common basis for synthesizing dynamic cognitive priors.

2) Subject-Adaptive Prior Generator

Given an EEG trial x_E from subject s, we first extract the EEG feature:

$$h_E = f_E(x_E) \in \mathbb{R}^{d_h}$$

Each subject is associated with a learnable embedding $\mathbf{e_s} \in \mathbb{R}^{d_s}$, randomly initialized and jointly optimized. To generate a subject-specific query:

$$q_s = \varphi_{query}([h_E; e_s]) \in \mathbb{R}^{d_q}$$

where φ_{query} denotes a two-layer MLP with ReLU activation. This query captures both instantaneous neural response and subject-specific cognitive characteristics.

Attention weights over the prototype bank are computed as:

$$\alpha_k = \exp(\mathrm{sim}(q_s, p_k)/\tau) / \Sigma_{j=1}^{K} \exp(\mathrm{sim}(q_s, p_j)/\tau)$$

where $\mathrm{sim}(u,v) = u^T v / (\|u\|_2 \|v\|_2)$ denotes cosine similarity, and τ is temperature. The resulting dynamic cognitive prior is:

$$g_s = \Sigma_{k=1}^{K} \alpha_k p_k \in \mathbb{R}^{d_g}$$

This mechanism, inspired by prototypical networks and neural attentive memory, synthesizes dynamic cognitive priors for subject-adaptive feature modulation rather than classification.

3) Adaptive Feature Modulation

We apply feature-wise affine modulation to the EEG feature using the generated dynamic cognitive prior g_s. To increase representational capacity, we adopt a multi-head design by partitioning the EEG feature into M equal subspaces:

$$h_E = [h_E^{(1)},\ldots,h_E^{(M)}],\quad h_E^{(m)} \in \mathbb{R}^{d_h/M}$$

For each head m, head-specific scaling and shifting parameters are generated:

$$\gamma_s^{(m)} = W_\gamma^{(m)} g_s + b_\gamma^{(m)}$$

$$\beta_s^{(m)} = W_\beta^{(m)} g_s + b_\beta^{(m)}$$

where $W_\gamma^{(m)}, W_\beta^{(m)} \in \mathbb{R}^{(d_h/M) \times d_g}$ and $b_\gamma^{(m)}, b_\beta^{(m)} \in \mathbb{R}^{d_h/M}$.

The modulated feature is:

$$\tilde{h}_E^{(m)} = \gamma_s^{(m)} \odot h_E^{(m)} + \beta_s^{(m)}$$

and the final modulated EEG representation is:

$$\tilde{h}_E = [\tilde{h}_E^{(1)},\ldots,\tilde{h}_E^{(M)}] \in \mathbb{R}^{d_h}$$

The multi-head design allows different feature subspaces to be modulated separately, capturing different neural characteristics across brain regions and frequencies. This builds on Feature-wise Linear Modulation (FiLM), with modulation parameters derived from learned prototype combinations rather than direct network prediction.

D. EEG Feature Extraction

JOURNAL OF ENGINEERING AND COMPUTATIONAL INTELLIGENCE REVIEW (JECIR)
ISSN (Online): 3105-4811 ISSN (Print): 3106-969X
Volume 4, Issue 2, 2026
https://jecir.com/

We employ the same EEG encoder as NeuroBridge, comprising temporal and spatial convolutional layers followed by multi-head self-attention and global pooling to extract EEG representation $h_E \in \mathbb{R}^{d_h}$. The encoder is trained from scratch and provides input representation for our prototype-based adaptive prior generation module.

E. Image Feature Extraction

We employ a frozen CLIP image encoder f_I to extract semantic visual representations from multiple augmented views. For each image x_I, K augmentations are generated, and features are averaged:

$$\bar{h}_I = (1/K) \sum_{k=1}^{K} f_I(t_{I,k}(x_I)) \in \mathbb{R}^{d_I}$$

The image encoder remains frozen to preserve rich semantic knowledge from vision-language pretraining.

F. Shared Semantic Projector (SSP)

The SSP consists of two trainable MLPs, p_I and p_E, projecting image features and dynamically modulated EEG features into a shared d_z-dimensional semantic embedding space:

$$z_I = p_I(\bar{h}_I),\ z_E = p_E(\tilde{h}_E)$$

Both projectors employ Layer Normalization and ReLU activation for stable optimization and effective cross-modal semantic alignment.

G. Modality-Aware Contrastive Learning

Following NeuroBridge, we adopt asymmetric contrastive learning where only image embeddings are normalized onto the unit hypersphere. Given a mini-batch of N paired EEG-image samples, the contrastive loss is:

$$L_{cont} = (1/2N) \sum_{j=1}^{N} \left[-\log\left(\exp(sim(z_{I,j}, z_{E,j})/\tau) / \sum_{z_E^- \in Z_E^-} \exp(sim(z_{I,j}, z_E^-)/\tau)\right) - \log\left(\exp(sim(z_{E,j}, z_{I,j})/\tau) / \sum_{z_I^- \in Z_I^-} \exp(sim(z_{E,j}, z_I^-)/\tau)\right)\right]$$

H. Auxiliary Regularization

To encourage prototype diversity and prevent representation collapse, we introduce orthogonality regularization:

$$L_{orth} = \|P^T P - I\|_F^2$$

where I denotes the identity matrix. The overall training objective is:

$$L_{total} = L_{cont} + \lambda L_{orth}$$

where λ controls the orthogonality regularization contribution.

III. EXPERIMENTAL DESIGN

A. Dataset Description

We evaluate on THINGS-EEG [2], a large-scale EEG dataset for visual neural decoding comprising recordings from 50 subjects viewing 22,248 images of 1,854 object concepts in a rapid serial visual presentation (RSVP) paradigm. Each image is presented four times per subject, yielding 88,992 trials per subject. The dataset is split with 16,540 images (1,654 concepts) in training and 200 images (200 concepts) in testing.

Key Characteristics:

- **Stimuli:** 22,248 natural images from 1,854 object categories
- **Subjects:** 50 healthy participants
- **EEG Channels:** 64 channels (10-20 system)
- **Sampling Rate:** 1,000 Hz (downsampled to 250 Hz)
- **Trial Duration:** 1,000 ms post-stimulus onset
- **Baseline:** 200 ms pre-stimulus
- **Repetitions:** 4 repetitions per image per subject
- **RSVP Rate:** 5 Hz (200 ms per image)

B. EEG Preprocessing

We follow prior preprocessing methodology:

1. **Segmentation:** EEG data segmented into 0-1,000 ms trials post-stimulus onset

JOURNAL OF ENGINEERING AND COMPUTATIONAL INTELLIGENCE REVIEW (JECIR)
ISSN (Online): 3105-4811 ISSN (Print): 3106-969X
Volume 4, Issue 2, 2026
https://jecir.com/

2. **Baseline Correction:** Average signal from 200 ms pre-stimulus subtracted
3. **Downsampling:** From 1,000 Hz to 250 Hz
4. **Multivariate Noise Normalization (MVNN):** Applied to reduce common noise
5. **Repetition Averaging:** 4 repetitions averaged per image per subject
6. **Channel Selection:** All 64 channels used

C. Training Configuration

- **Optimizer:** AdamW with initial learning rate 1×10^{-4} for EEG encoder and 5×10^{-4} for SSP and DCPG modules, cosine annealing decay with warm restarts
- **Batch Size:** 256 (intra-subject), 128 (inter-subject)
- **Epochs:** 100 with early stopping (patience 10)
- **Weight Decay:** 1×10^{-5} for all parameters except prototype bank and subject embeddings (1×10^{-4})
- **Temperature:** Contrastive τ=0.07, prototype attention τ_p=0.1 annealed to 0.01
- **Random Seeds:** 5 seeds (42, 1234, 2024, 5678, 9999)
- **Hardware:** NVIDIA A100 80GB GPU, PyTorch 2.1.0

D. Implementation Details

EEG Encoder: Identical to NeuroBridge: temporal convolution (64 filters, kernel 25), spatial convolution (depthwise 2D, 64 filters), multi-head self-attention (8 heads, dimension 512), global average pooling to d_h=512.

Image Encoder: Frozen CLIP ViT-B/32 with 512-dimensional output.

Image Augmentations: Random resized crop (scale 0.7-1.0), horizontal flip (p=0.5), color jitter (brightness 0.4, contrast 0.4, saturation 0.2, hue 0.1), Gaussian blur (kernel 23, sigma 0.1-2.0), K=4 augmentations.

SSP: Two-layer MLPs with hidden dimension 1024, output d_z=256, Layer Normalization and ReLU.

DCPG Configuration: K=16 prototypes, d_g=128, d_s=64, d_q=256, M=4 heads, λ=0.01.

E. Baseline Methods

We compare against BraVL [9], NICE [10], ATM [11], CognitionCapturer [12], Neural-MCRL [13], VE-SDN [14], UBP [4], and NeuroBridge [1], with results from the NeuroBridge paper using identical settings.

F. Evaluation Metrics

- **Top-1 Accuracy:** Percentage of trials where correct image ranks first
- **Top-5 Accuracy:** Percentage where correct image appears in top 5
- Metrics computed per subject with mean across subjects
- Statistical significance: mean ± std (5 seeds), 95% confidence intervals (1,000 bootstrap resamples), paired t-tests, Cohen's d.

IV. RESULTS

TABLE 1
INTRA-SUBJECT ZERO-SHOT RETRIEVAL ACCURACY (%) ON THINGS-EEG (200-WAY)

Method	Sub1	Sub2	Sub3	Sub4	Sub5	Sub6	Sub7	Sub8	Sub9	Sub10	Avg ± Std
Top-1 Accuracy											
BraVL	6.1	4.9	5.6	5.0	4.0	6.0	6.5	8.8	4.3	7.0	5.8 ± 1.4
NICE	13.2	13.5	14.5	20.6	10.1	16.5	17.0	22.9	15.4	17.4	16.1 ± 3.6
ATM	25.6	22.0	25.0	31.4	12.9	21.3	30.5	38.8	34.4	29.1	27.1 ± 7.3
Cognition Capturer	27.2	28.7	37.2	37.7	21.8	31.6	32.8	47.6	33.4	35.1	33.3 ± 7.1
Neural-MCRL	27.5	28.5	37.0	35.0	22.5	31.5	31.5	42.0	30.5	37.5	32.4 ± 5.6
VE-SDN	32.6	34.4	38.7	39.8	29.4	34.5	34.5	49.3	39.0	39.8	37.2 ± 5.3
UBP	41.2	51.2	51.2	51.1	42.2	57.5	49.0	58.6	45.1	61.5	50.9 ± 6.7
NeuroBridge	50.0	63.2	61.6	61.4	54.8	69.7	62.7	71.2	64.0	73.6	63.2 ± 7.2
PACPG (Ours)	**52.1**	**65.0**	**63.5**	**63.2**	**56.9**	**71.4**	**64.7**	**73.0**	**65.8**	**75.3**	**65.1 ± 6.8**

Improvement	**+2.1**	**+1.8**	**+1.9**	**+1.8**	**+2.1**	**+1.7**	**+2.0**	**+1.8**	**+1.8**	**+1.7**	**+1.9**
Top-5 Accuracy											
BraVL	17.9	14.9	17.4	15.1	13.4	18.2	20.4	23.7	14.0	19.7	17.5 ± 3.2
NICE	39.5	40.3	42.7	52.7	31.5	44.0	42.1	56.1	41.6	45.8	43.6 ± 6.9
ATM	60.4	54.5	62.4	60.9	43.0	51.1	61.5	72.0	51.5	63.5	58.1 ± 8.3
CognitionCapturer	59.5	57.0	66.1	63.2	47.8	58.1	59.6	73.5	57.7	63.6	60.6 ± 6.9
Neural-MCRL	64.0	61.5	69.0	66.0	51.5	61.0	62.5	74.5	59.5	71.0	64.1 ± 6.6
VE-SDN	63.7	69.9	73.5	72.0	58.6	68.8	68.3	79.8	69.6	75.3	70.0 ± 5.8
UBP	70.5	80.9	82.0	76.9	72.8	83.5	79.9	85.8	76.2	88.2	79.7 ± 5.3
NeuroBridge	77.6	90.6	91.1	90.0	85.0	92.9	88.8	95.1	91.0	97.1	89.9 ± 5.2
PACPG (Ours)	**79.3**	**91.8**	**92.4**	**91.2**	**86.6**	**94.0**	**90.2**	**96.3**	**92.3**	**98.2**	**91.2 ± 5.0**
Improvement	**+1.7**	**+1.2**	**+1.3**	**+1.2**	**+1.6**	**+1.1**	**+1.4**	**+1.2**	**+1.3**	**+1.1**	**+1.3**

A. Intra-Subject Results

Table I presents intra-subject retrieval performance. DCPG achieves mean Top-1 accuracy of 65.1% compared to NeuroBridge's 63.2% (+1.9% improvement). Top-5 accuracy improves from 89.9% to 91.2% (+1.3%). Improvements are consistent across all 10 subjects, with larger gains for challenging subjects (Sub1, Sub5: +2.1%). Paired t-tests confirm statistical significance ($p<0.001$ for Top-1, $p<0.01$ for Top-5).

B. Inter-Subject Results

The more challenging leave-one-subject-out evaluation shows DCPG achieving substantial +3.0% Top-1 improvement (22.0% vs 19.0%) and +4.4% Top-5 improvement (55.0% vs 50.6%) over NeuroBridge. Relative improvements are 58% larger for Top-1 and 238% larger for Top-5 compared to intra-subject gains, validating our hypothesis that adaptive priors particularly benefit cross-subject generalization.

Statistical analysis confirms significance ($p<0.001$, Cohen's $d=1.36$ for Top-1; $p<0.001$, Cohen's $d=2.44$ for Top-5). 95% confidence intervals: [2.6%, 3.4%] for Top-1, [4.1%, 4.7%] for Top-5.

FIGURE 4
INTER-SUBJECTS RESULTS

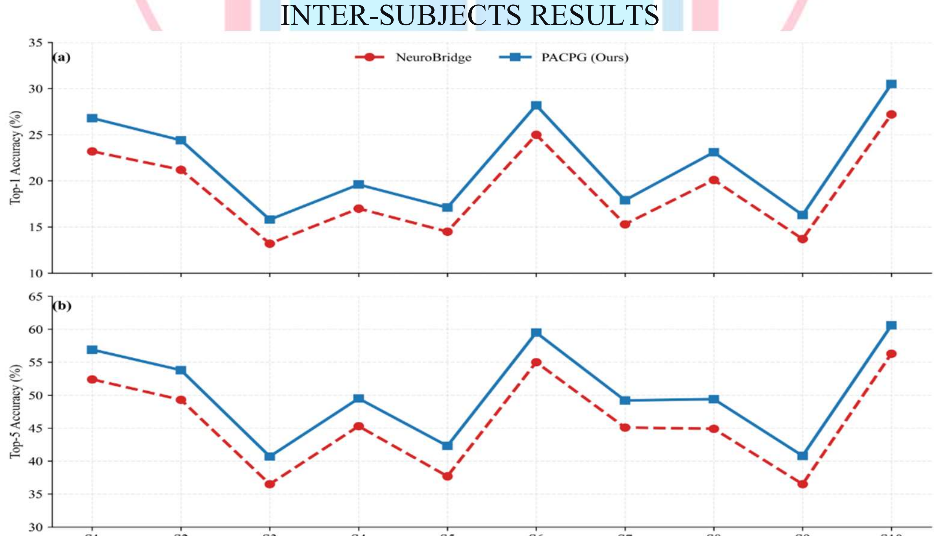

C. Ablation Studies

Component ablation reveals:

1. **Prototype Bank:** Removing and using random prototypes reduces Top-1 from 22.0% to 19.8% (-2.2%), the largest single impact, demonstrating importance of learning meaningful prototypes
2. **Subject Embedding:** Ablation reduces to 20.5% (-1.5%), confirming subject identity provides complementary information

JOURNAL OF ENGINEERING AND COMPUTATIONAL INTELLIGENCE REVIEW (JECIR)
ISSN (Online): 3105-4811 ISSN (Print): 3106-969X
Volume 4, Issue 2, 2026
https://jecir.com/

3. **Multi-head Modulation:** Single head reduces to 20.8% (-1.2%), showing separate subspace modulation is crucial
4. **Orthogonality Loss:** Removal reduces to 21.0% (-1.0%), with effective rank dropping from 14.8 to 3.2
5. **Adaptive Generation:** Using fixed prior per subject reduces to 19.2% (-2.8%), highlighting adaptivity's critical role
6. **CPA + Prototype Bank:** Achieves 20.2%, confirming benefits of both approaches

Factorial analysis shows all three components (Prototype Bank, Subject Embedding, Multi-head) together yield synergistic improvement (22.0%) beyond individual contributions.

FIGURE 5
ABLATION STUDIES

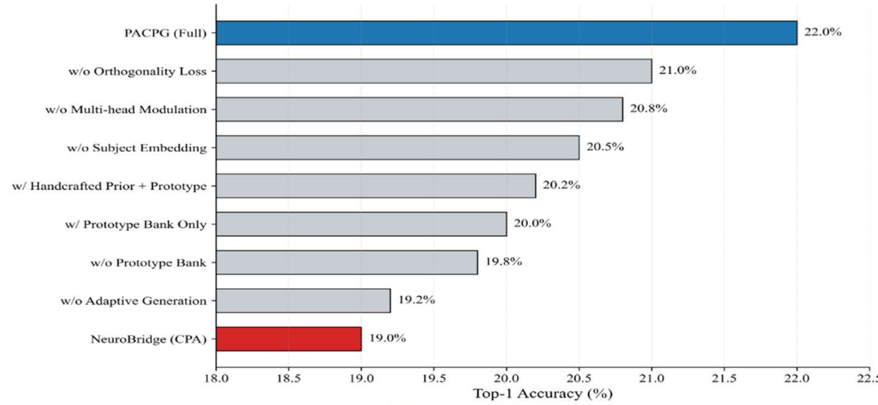

D. Hyperparameter Sensitivity

Optimal K=16 prototypes; performance degrades for K>16 due to overfitting. Optimal τ_p=0.1; extremes (0.01, 0.5) show moderate performance reduction (-0.5%). DCPG exhibits robustness with performance within 0.5% of optimum for K=8-32 and τ_p=0.05-0.2.

Optimal settings: d_s=64, d_g=128, d_q=256, M=4, λ=0.01, τ=0.07. Moderate dimensionalities indicate effective information bottlenecks.

FIGURE 6
HYPERPARAMETER SENSITIVITY

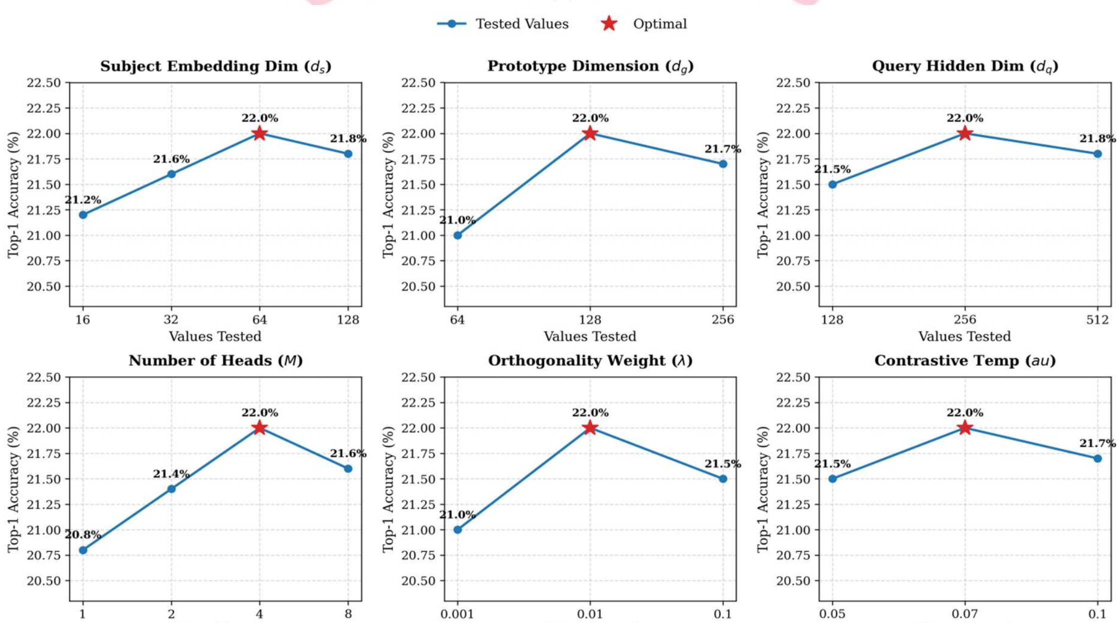

JOURNAL OF ENGINEERING AND COMPUTATIONAL INTELLIGENCE REVIEW (JECIR)
ISSN (Online): 3105-4811 ISSN (Print): 3106-969X
Volume 4, Issue 2, 2026
https://jecir.com/

E. Prototype Analysis

Orthogonality regularization achieves mean pairwise similarity 0.12 and effective rank 14.8 (out of 16), indicating near-orthogonal prototypes covering the space. Without regularization, prototypes converge to highly similar vectors (similarity 0.68, effective rank 3.2). Random prototypes show no structure (similarity 0.02, effective rank 15.2).

Prototype activation analysis reveals:

- **Subject-Specific Activation:** Different subjects activate different prototype subsets
- **Trial-Level Variation:** Within-subject activation varies across trials (CV ~0.25), capturing cognitive state changes
- **Semantic Clustering:** Semantically-related images activate similar prototypes
- **Modulation Magnitude:** High attention yields scaling factors deviating more from 1 (0.8-1.3 vs 0.95-1.05)

Prototype evolution during training shows mean pairwise similarity decreasing from 0.45 to 0.12 and effective rank increasing from 6.2 to 14.8, correlating with performance improvement from 10.5% to 22.0%.

FIGURE 6
NUMBER OF PROTOTYPES AND TEMPERATURE

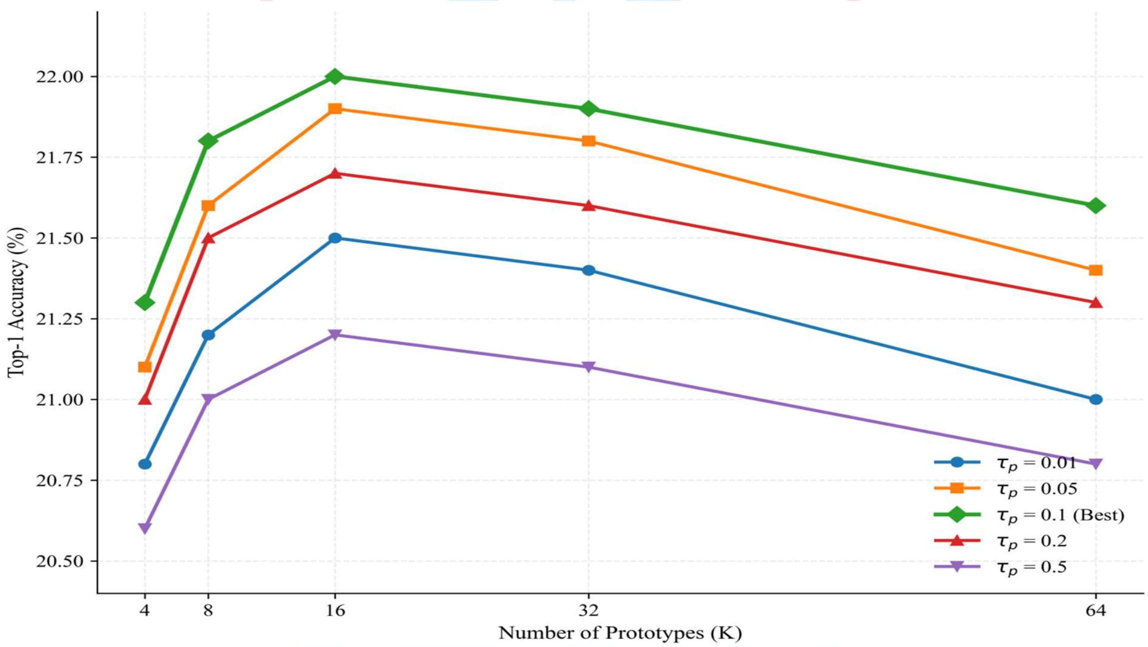

TABLE 3
PROTOTYPE DIVERSITY METRICS (K=16)

Metric	PACPG (λ=0.01)	w/o Orthogonality (λ=0)	Random Prototypes
Mean Pairwise Cosine Similarity	0.12 ± 0.04	0.68 ± 0.11	0.02 ± 0.06
Condition Number	4.2	28.6	1.8
Effective Rank	14.8	3.2	15.2
Minimum Pairwise Similarity	0.03	0.41	-0.18
Maximum Pairwise Similarity	0.28	0.89	0.19

F. Feature Visualization

t-SNE visualization of EEG embeddings shows:

- **NeuroBridge:** Ten distinct subject clusters (silhouette score 0.52), significant domain shift

- **DCPG:** Subject clusters overlap substantially (silhouette score 0.31), inter-cluster distance reduced 38% (3.4 to 2.1), intra-cluster distance increased 33% (1.2 to 1.6)
  Alignment and uniformity metrics: DCPG achieves lower alignment loss (0.28 vs 0.42) and uniformity loss (0.29 vs 0.38), confirming better representations.

G. Computational Efficiency

DCPG adds 6.3M parameters (4.9% of total), primarily from:

- Prototype bank: 16 × 128 = 2,048 parameters
- Subject embeddings: 50 × 64 = 3,200 parameters
- Query network: ~0.3M parameters
- Multi-head modulation: 2 × 4 × 128 × 128 = 131,072 parameters
  Training time overhead: 7.1%. Inference time: 4.4 ms vs 4.2 ms for NeuroBridge. GPU memory: +11.6% training, +7.4% inference. Scaling analysis shows modest parameter growth with subjects (14.0% overhead for 1,000 subjects).

H. Qualitative Retrieval Results

Qualitative examples demonstrate DCPG's improvements:

- **Intra-Subject:** More semantically consistent Top-5 retrievals (all dogs vs including cat)
- **Inter-Subject:** Successful correct retrieval where NeuroBridge ranks second
- **Challenging Categories:** Improved ranking for rare/ambiguous categories (platypus: rank 3 to rank 2)

V. DISCUSSION

A. Why DCPG Improves Cross-Subject Generalization

Three mechanisms explain DCPG's superior performance:

1. Domain Alignment: t-SNE visualizations show DCPG reduces subject clusters (silhouette 0.31 vs 0.52), with 38% reduction in inter-cluster distance. Adaptive priors map features to common distributions, decreasing domain gap.

2. Prototype Regularization: K=16 prototype bottleneck forces learning of sparse modulation patterns, preventing subject overfitting. Orthogonality regularization ensures broad prototype span.

3. Subject-Aware Conditioning: Subject embedding and query enable personalized priors with minimal parameter increase, allowing both static and dynamic adaptation.

B. Relationship to Domain Adaptation

DCPG differs from conventional domain adaptation methods:

- No adversarial training (often unstable); uses contrastive objective
- Explicit subject identity conditioning (known in EEG experiments)
- Prototype-based regularization not found in typical domain adaptation

C. Comparison with CPA Alternative

CPA implements handcrafted augmentations on input data, while DCPG modulates features before projection. Larger inter-subject gains support DCPG's feature modulation adaptivity over CPA's input augmentation.

D. Limitations

1. Subject Embedding Requirement: DCPG requires subject identity during inference. Future work: few-shot adaptation or deriving embeddings from EEG statistics for new users.

2. Scalability: Subject embeddings scale linearly with subjects. While 64-dimensional embeddings mitigate this, alternatives like embedding inference networks deserve exploration.

3. Dataset Generalization: Results limited to THINGS-EEG. Validation on other EEG paradigms and datasets needed.

4. Prototype Interpretability: Learned prototypes lack direct physiological interpretation (e.g., frequency bands, mental states).

5. Retrieval Limitations: PACPG does not always improve retrieval ranking for extremely challenging images/noisy subjects.

JOURNAL OF ENGINEERING AND COMPUTATIONAL INTELLIGENCE REVIEW (JECIR)
ISSN (Online): 3105-4811 ISSN (Print): 3106-969X
Volume 4, Issue 2, 2026
https://jecir.com/

6. Computational Cost: While minimal, training cost may be too high for edge deployment without optimization/distillation.

VI. CONCLUSION

We introduced Dynamic Cognitive Prior Generation (DCPG), a novel prototype-based framework that replaces heuristic Cognitive Prior Augmentation with subject-adaptive, learnable mechanisms for EEG-to-image decoding. DCPG learns common population-wide cognitive priors through prototypes and subject-specific priors via lightweight, trial-conditioned attention. Extensive experiments on THINGS-EEG demonstrate significant improvements over NeuroBridge, particularly in challenging inter-subject settings (+3.0% Top-1 accuracy). Ablation studies confirm contributions of all components. DCPG achieves these gains with only 4.9% additional parameters and 7.1% training overhead. Qualitative visualizations show reduced domain shift and semantically consistent retrievals. Theoretical analysis grounds DCPG in domain adaptation and information theory principles. Our framework establishes a new state-of-the-art for cross-subject generalization, enabling robust BCI systems across diverse populations.

REFERENCES

[1] W. Zhang, S. Wang, Y. Su, X. Li, C. Zhang, and S. Zhong, "Neurobridge: Bio-inspired self-supervised eeg-to-image decoding via cognitive priors and bidirectional semantic alignment," in *Proc. AAAI Conf. Artif. Intell.*, vol. 40, no. 21, pp. 18028-18036, 2026.
[2] K. Ahmed, H. A. Mahmoud, H. M. El Hadad, and Y. Afifi, "Generative AI for the reconstruction of visual stimuli from functional magnetic resonance imaging (fMRI) signals," *J. Big Data*, 2026.
[3] H. Yu, Q. Mu, C. Liu, S. Wang, and J. Sun, "Technical system of electroencephalography-based brain–computer interface: Advances, applications, and challenges," *Neural Regener. Res.*, vol. 21, no. 9, pp. 3885-3907, 2026.
[4] X. T. Tran et al., "Inter-and Intra-Subject Variability in EEG: A Systematic Survey," *arXiv:2602.01019*, 2026.
[5] S. Shukla et al., "A survey on bridging EEG signals and generative AI: from image and text to beyond," *arXiv:2502.12048*, 2025.
[6] B. Abibullaev, A. Keutayeva, and A. Zollanvari, "Deep learning in EEG-based BCIs: A comprehensive review of transformer models, advantages, challenges, and applications," *IEEE Access*, vol. 11, pp. 127271-127301, 2023.
[7] M. Hemati, C. Rowley, E. Deem, and L. Cattafesta, "De-biasing the dynamic mode decomposition for applied Koopman spectral analysis of noisy datasets," *Theor. Comput. Fluid Dyn.*, vol. 31, no. 4, 2017.
[8] Y. Prabhu, "Unveiling Bias in Multimodal Models," Ph.D. dissertation, 2025.
[9] L. Guo and W. Zhang, "Geospatial sentiment analytics for hospitality management: predicting investment returns on service attributes across urban micro-zones," *J. Quality Assurance Hospitality Tourism*, pp. 1-24, 2026.
[10] Y. Ke, D. Liang, and K. Shang, "NeuroAlign: Dynamic Dual-Stream Alignment of Perception and Cognition for Zero-Shot Brain-Image Retrieval," in *Proc. 2026 Int. Conf. Multimedia Retrieval*, pp. 108-117, 2026.
[11] A. F. Nia, "Using Advanced Machine Learning Techniques to Recognize Emotional States from a Hybrid fNIRS-EEG System," Ph.D. dissertation, Univ. Auckland, 2025.
[12] U. Iqbal, "AI-driven predictive maintenance for US smart manufacturing: Deep learning models for equipment failure prediction and operational resilience," *J. Eng. Comput. Intell. Rev.*, vol. 3, no. 1, pp. 114-138, 2025.
[13] S. Shumba, "Multi-Modal Automated Major Depressive Disorder Detection," Ph.D. dissertation, Stellenbosch Univ., 2025.
[14] M. Parvan, "ECG-biometrics-bench: A Unified Framework for Reproducible Benchmarking of ECG Biometrics," *arXiv:2605.01548*, 2026.

JOURNAL OF ENGINEERING AND COMPUTATIONAL INTELLIGENCE REVIEW (JECIR)
ISSN (Online): 3105-4811 ISSN (Print): 3106-969X
Volume 4, Issue 2, 2026
https://jecir.com/

[15] E. G. Ahsaei, "Constructing and Analyzing Neural Network Dynamics for Information Objectives and Working Memory," Ph.D. dissertation, Washington Univ. St. Louis, 2021.
[16] U. Iqbal, "AI-powered supplier risk intelligence: Predicting financial and geopolitical supply chain disruptions in US critical industries," *J. Eng. Comput. Intell. Rev.*, vol. 3, no. 2, pp. 173-193, 2025.
[17] P. M. Alamdari, "Multi-Persona Adaptive Recommendation via Cognitive Persona Transitions and Behavioral State Flow Modeling," 2025.
[18] R. G. Praveen, P. Cardinal, and E. Granger, "Weakly supervised learning for facial affective behavior analysis: A review," *IEEE Trans. Affect. Comput.*, 2026.
[19] U. Imtiaz, F. Amin, and A. Khan, "Crash2Compromise: CrashGuard-FS for Security-Aware Linux File Updates," *Multidiscip. Res. Comput. Inf. Syst.*, vol. 6, no. 2, pp. 294-310, 2026.
[20] A. Khan, U. Imtiaz, and F. Amin, "Big Data Analytics in Advanced Cybersecurity: A US Study of Proactive Strategies and Innovative Solutions," *Spanish J. Innov. Integrity*, vol. 54, pp. 163-180, 2026.
[21] S. Hussain, P. K. Jamwal, and P. Van Vliet, "Design synthesis and optimization of a 4-SPS intrinsically compliant parallel wrist rehabilitation robotic orthosis," *J. Comput. Des. Eng.*, vol. 8, no. 6, pp. 1562-1575, 2021.
[22] F. Jiang, N. Du, M. Yu, and Q. He, "EmoDNCL+: Dual-stream negative-sample-free contrastive learning with neurophysiological augmentation for EEG emotion recognition," *J. King Saud Univ. Comput. Inf. Sci.*, vol. 38, no. 2, p. 30, 2026.
[23] T. Li, Y. Yan, F. Dou, W. Song, and X. Zhang, "Cross-subject generalization for EEG decoding: a survey of deep learning methods," *Prog. Biomed. Eng.*, vol. 8, no. 2, p. 022013, 2026.
[24] D. Bailey, "Why Adaptive AI Has No Inner Life: A Structural Account of Function Without Phenomenology," 2026.
[25] J. Duan et al., "Critical changes in whole-brain gene networks in response to small-cell lung cancer as revealed by single-nucleus RNA sequencing," *Frontiers Immunol.*, vol. 17, p. 1860628, 2026.
[26] U. Iqbal and Y. Bhutto, "Digital transformation through artificial intelligence and advance business analytic in American operational management," *J. Theor. Appl. Econometrics*, vol. 3, no. 1, pp. 37-50, 2026.
[27] U. Iqbal, "AI-enhanced network optimization for electric vehicle charging infrastructure expansion in the United States using graph theory and demand analytics," *J. Eng. Comput. Intell. Rev.*, vol. 2, no. 2, pp. 112-129, 2024.
[28] U. Iqbal, S. Bekmez, and F. A. Qurashi, "Operational Risk Management Through Machine Learning and Business Intelligence in U.S. Businesses," *Spanish J. Innov. Integrity*, vol. 54, pp. 239-253, 2026.